JOURNAL OF BACTERIOLOGY, Jan. 2001, p. 270–279 Vol. 183, No. 1
0021-9193/01/$04.00+0 DOI: 10.1128/JB.183-1.270–279.2001

Transcriptional Organization and Dynamic Expression of the *hbpCAD* Genes, Which Encode the First Three Enzymes for 2-Hydroxybiphenyl Degradation in *Pseudomonas azelaica* HBP1

MARCO C. M. JASPERS,[1] ANDREAS SCHMID,[2] MARK H. J. STURME,[1]† DAVID A. M. GOSLINGS,[1]‡ HANS-PETER E. KOHLER,[1] AND JAN ROELOF VAN DER MEER[1]*

Swiss Federal Institute for Environmental Science and Technology and Swiss Federal Institute of Technology, CH-8600 Dübendorf,[1] and Institute of Biotechnology, Swiss Federal Institute of Technology, CH-8093 Zürich,[2] Switzerland

Received 3 August 2000/Accepted 6 October 2000

Pseudomonas azelaica* HBP1 degrades the toxic substance 2-hydroxybiphenyl (2-HBP) by means of three enzymes that are encoded by structural genes *hbpC*, *hbpA*, and *hbpD*. These three genes form a small noncontiguous cluster. Their expression is activated by the product of regulatory gene *hbpR*, which is located directly upstream of the *hbpCAD* genes. The HbpR protein is a transcription activator and belongs to the so-called XylR/DmpR subclass within the NtrC family of transcriptional activators. Transcriptional fusions between the different *hbp* intergenic regions and the *luxAB* genes of *Vibrio harveyi* in *P. azelaica* and in *Escherichia coli* revealed the existence of two HbpR-regulated promoters; one is located in front of *hbpC*, and the other one is located in front of *hbpD*. Northern analysis confirmed that the *hbpC* and *hbpA* genes are cotranscribed, whereas the *hbpD* gene is transcribed separately. No transcripts comprising the entire *hbpCAD* cluster were detected, indicating that transcription from P_{hbpC} is terminated after the *hbpA* gene. *E. coli* mutant strains lacking the structural genes for the RNA polymerase σ^{54} subunit or for the integration host factor failed to express bioluminescence from P_{hbpC}- and P_{hbpD}-*luxAB* fusions when a functional *hbpR* gene was provided in *trans*. This pointed to the active role of σ^{54} and integration host factor in transcriptional activation from these promoters. Primer extension analysis revealed that both P_{hbpC} and P_{hbpD} contain the typical motifs at position −24 (GG) and −12 (GC) found in σ^{54}-dependent promoters. Analysis of changes in the synthesis of the *hbp* mRNAs, in activities of the 2-HBP pathway enzymes, and in concentrations of 2-HBP intermediates during the first 4 h after induction of continuously grown *P. azelaica* cells with 2-HBP demonstrated that the specific transcriptional organization of the *hbp* genes ensured smooth pathway expression.

The *hbp* genes allow *Pseudomonas azelaica* strain HBP1 to metabolize the toxic compounds 2-hydroxybiphenyl (2-HBP) and 2,2′-dihydroxybiphenyl (2,2′-DHBP) (21, 22, 44). The *hbp* system consists of three structural genes, *hbpC*, *hbpA*, and *hbpD*, which encode the enzymes for the first steps of 2-HBP degradation (Fig. 1), and of the regulatory gene *hbpR* (20, 44). Expression of the 2-HBP pathway is tightly regulated, and the respective enzyme activities can only be measured when cells are induced with 2-HBP or 2,2′-DHBP (20, 22). By using knockout studies and complementation assays we identified the HbpR protein as the key regulator for 2-HBP pathway expression (20).

On the basis of sequence comparisons, the HbpR protein belongs to the NtrC family of prokaryotic transcriptional activators (20). Members of this family specifically bind to (nearly) palindromic DNA sequences located around 100 to 200 bp upstream of their target promoters (the so-called bacterial enhancer-like elements or upstream activating sequences [UASs]) (reviewed in references 25 and 29). Transcriptional activation by NtrC-type regulators occurs through specific biochemical or physiological stimuli which may change the protein's conformation and which may provoke multimerizations, eventually triggering an ATPase activity (29, 34, 38). The ATPase activity is needed for catalyzing the formation of the open transcriptional complex by σ^{54}-containing RNA polymerase (RNAP) (25) at promoters with a −24 (GG)/−12 (GC) motif (26). Histone-like proteins such as integration host factor (IHF) and protein HU may assist in the process of transcriptional activation. IHF binds DNA specifically while introducing strong hinge-like bends of 140° or greater, whereas HU binds DNA aspecifically and increases the flexibility of the bound DNA (reviewed in reference 31). IHF and HU are capable of establishing a particular geometry at the promoter DNA which may enable a bound NtrC-type activator at the UASs to contact promoter-bound RNAP-σ^{54} (12, 18, 37). For XylR and its P_u promoter, IHF was even shown to promote a better recruitment of σ^{54}-RNAP to the −24/−12 promoter by providing additional contacts between the α subunit of the holoenzyme and an otherwise-distant *cis* element (UP-like element) (8, 10, 41).

One subclass within the NtrC family, the XylR/DmpR subclass, is formed by regulatory proteins which are activated by direct interaction with aromatic effector compounds without

* Corresponding author. Mailing address: EAWAG, Ueberlandstrasse 133, Postfach 611, CH-8600 Duebendorf, Switzerland. Phone: 41-1-823 54 38. Fax: 41-1-823 55 47. E-mail: vdmeer@eawag.ch.

† Present address: Department of Microbiology, Wageningen Agricultural University, Wageningen, The Netherlands.

‡ Present address: Institute for Plant Science, Swiss Federal Institute of Technology, CH-8092 Zürich, Switzerland.

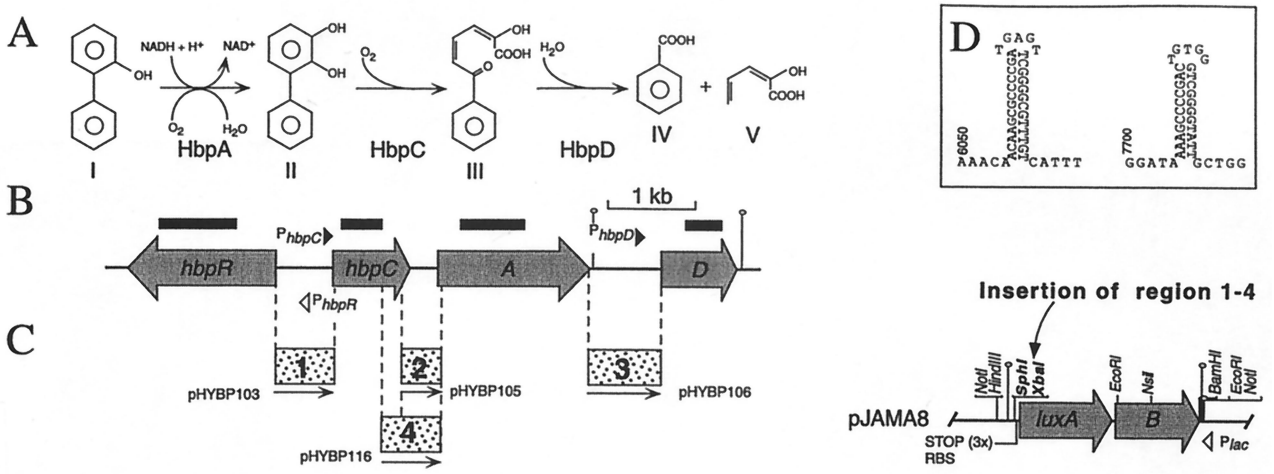

FIG. 1. (A) Initial metabolism of 2-HBP and 2,2′-DHBP in *P. azelaica* HBP1. The enzymes responsible for catalyzing the different reactions are indicated below each conversion step. HbpA catalyzes the NADH-dependent *ortho* hydroxylation of 2-HBP (I) to 2,3-dihydroxybiphenyl (II) (21, 22, 48). HbpC catalyzes the cleaving of 2,3-dihydroxybiphenyl at a *meta* position, which results in 2-hydroxy-6-oxo-6-phenyl-2,4-hexadienoic acid (III) (22, 44). This compound is then hydrolyzed by HbpD to benzoic acid and 2-hydroxy-2,4-pentadienoic acid (IV and V) (22). (B) Genetic organization of the *hbp* genes. Shaded arrows, orientations and sizes of the genes; solid line, noncoding DNA; black bars, DNA fragments used as probes in the Northern analysis. Hairpin-like structures indicate the relative locations of predicted terminators. (C) (Left) Fragments used for transcriptional fusions with *luxAB* in pJAMA8 (resulting plasmid names are indicated). (Right) Restriction map of plasmid pJAMA8. The unique *Sph*I and *Xba*I sites used for cloning are in boldface. The locations of other relevant restriction sites and the orientation of the *lac* promoter are indicated. RBS, ribosome binding site; STOP (3×), stop codons in all three reading frames. Solid line, vector-derived DNA. (D) ρ-independent transcription terminator structures predicted from the DNA sequence downstream of *hbpA* (position 6050 of the sequence with GenBank accession no. U73900) and *hbpD* (position 7700).

the need for a sensor kinase component (reviewed in reference 45). These NtrC-type monocomponent regulators exhibit a modular design. The N-terminal A domain recognizes the effector, the central C domain is essential for the different steps needed in transcriptional activation (ATP binding and hydrolysis, oligomerization, and contacting RNAP-σ^{54}), and the C-terminal D domain binds to the DNA at the UASs by means of a helix-turn-helix motif (reviewed in reference 29). In the current model for activation, the A domain acts as a specific interdomain inhibitor which occludes the otherwise constitutive ATPase activity of the central C domain (13, 32, 33). The binding of an effector molecule leads to a conformational change in the A domain which is transmitted through a short flexible interdomain linker hinge region, the Q linker (52), in such a way that the inhibition of ATPase activity of the C domain is released (45).

Based on sequence homology and the capability to interact directly with 2-HBP and other aromatic effectors, HbpR could be assigned to the XylR/DmpR subclass (20). Within this group, HbpR takes a distinct position since it is activated by bicyclic structures, such as 2-HBP and 2,2′-DHBP and the structural analogs 2-aminobiphenyl and 2-hydroxybiphenylmethane (20). Monoaromatic compounds are not effectors for HbpR-mediated transcriptional activation (20).

Here we report on the transcriptional organization of the *hbpCAD* genes, which is rather unusual for *Pseudomonas* catabolic genes. By using promoter fusion studies, primer extension experiments, and Northern analysis, we discovered two separately regulated operons within the *hbpCAD* gene cluster. The expression of both operons is mediated by HbpR and requires RNAP-σ^{54} and IHF for full activation. From observations of the first stages of induction of the 2-HBP pathway in chemostat-grown *P. azelaica* cells, we discuss how the present transcriptional organization effects expression of the *hbp* genes for achieving 2-HBP degradation.

MATERIALS AND METHODS

Bacterial strains and culture conditions. The bacterial strains used in this study are listed in Table 1. *P. azelaica* HBP1 is able to use 2-HBP and 2,2′-DHBP as a sole source of carbon and energy (21). *P. azelaica* strains HBP104 (20), HBP107, HBP108, and HBP118 originate from strain HBP1 and contain transcriptional fusions between the different intergenic regions of the *hbp* structural genes and the *luxAB* genes (Fig. 1C) integrated on the chromosome in monocopy.

Escherichia coli strains were grown at 37°C on Luria-Bertani medium (42). *P. azelaica* strains were routinely grown at 30°C on *Pseudomonas* mineral medium (MM) (16) containing 10 mM succinate or 2.9 mM 2-HBP. When required the media were supplemented with antibiotics as described before (20).

Chemostat cultivation of *P. azelaica* HBP1 and RNA isolation. *P. azelaica* HBP1 was continuously cultivated in a 2.5-liter reactor (MBR, Wetzikon, Switzerland). Culture conditions were, in short, a dilution rate of 0.085 h^{-1} under carbon-limited conditions, a temperature of 30°C, an operating volume of the reactor of 1.2 liters, pH 6.8, and a stirring velocity of 450 rpm. To all media, silicon antifoam was added at a final concentration of 100 ppm. Growth medium for noninducing conditions was based on MM containing 20 mM glucose, on which the cells were grown for about eight volume changes before being induced. Optical density at 600 nm of the culture at steady state was 2.6. Induction was achieved by adding 0.24 ml from a 2.5 M 2-HBP solution in dimethyl sulfoxide (DMSO) and simultaneously shifting the feed medium to MM with 20 mM glucose and 0.5 mM 2-HBP.

Total RNA from *P. azelaica* HBP1 was isolated from the chemostat 1 min before shifting to 2-HBP-containing medium and 3, 7, 13, 23, and 30 min after the shift. Three-milliliter samples were taken directly from the chemostat, and cells were immediately pelleted by centrifugation (15,000 × *g*, 30 s) at 4°C. Total RNA was then isolated as described previously (6) and treated with DNase I (RNase free; Boehringer GmbH, Mannheim, Germany). RNA concentrations were determined spectrophotometrically by measuring the optical density at 260 nm in a Uvikon 800 spectrophotometer (Kontron Instruments AG, Zürich, Switzerland).

TABLE 1. Bacterial strains used in this work

Strain	Relevant genotype or characteristics[a]	Source or reference
E. coli		
CC118λ*pir*	Host strain to propagate plasmids with an R6K origin of replication	17
DH5α	Host strain in routine cloning experiments	Gibco BRL, Life Technologies
N99	*galK*	28
A5196	Cm^r Km^r; N99 *hupA16*::Kan *hupB11*::Cat; derivative of strain N99 lacking the α and β subunits of HU	28
A5475	N99 Δ*himA82 hip157*; derivative of strain N99 lacking the α and β subunits of IHF	28
ET8000	*rbs lacZ*::IS*1 gyrA hutC*$_K$(Con)	27
ET8045	Tc^r; ET8000 *rpoN208*::Tn*10*; derivative of strain ET8000 lacking the σ^{54} subunit	27
P. azelaica		
HBP1	2-HBP^+; wild type	21
HBP104	Km^r; 2-HBP^+; contains mini-Tn*5* (region 1 [P_{hbpC}]-*luxAB res-npt-res*) of plasmid pHYBP104	20
HBP107	Km^r; 2-HBP^+; contains mini-Tn*5* (region 2-*luxAB res-npt-res*) of plasmid pHYBP107	This work
HBP108	Km^r; 2-HBP^+; contains mini-Tn*5* (region 3 [P_{hbpD}]-*luxAB res-npt-res*) of plasmid pHYBP108	This work
HBP118	Km^r; 2-HBP^+; contains mini-Tn*5* (region 4-*luxAB res-npt-res*) of plasmid pHYBP118	This work
HBP104121	Km^r Sm^r Tc^r; 2-HBP^-; derivative of strain HBP104 with disrupted *hbpR*	20
HBP108121	Km^r $Sm^r$$Tc^r$; 2-$HBP^-$; derivative of strain HBP108 with disrupted *hbpR*	This work

[a] 2-HBP^+, ability to grow on 2-HBP; 2-HBP^-, inability to grow on 2-HBP; *res-npt-res*, element with kanamycin resistance gene of Tn*5* (*npt*) flanked by tandem multimer resolution sequences (*res*) of RP4 (24); regions 1 to 4 correspond to the *hbp*-derived intergenic regions as shown in Fig. 1C.

Recombinant DNA techniques, DNA sequencing, and Southern analysis. Plasmid DNA isolations, ligations, transformations, PCR, and other DNA manipulations were carried out according to well-established procedures (4, 42) or as described previously (20). Double-stranded template sequencing was performed with primers that were labeled with fluorescent dye IRD-800 or IRD-700 at the 5′ end, as described elsewhere (40).

Chromosomal insertions of mini-Tn*5* derivatives or homologous recombined DNA into the *P. azelaica* chromosome were verified by Southern analysis. DNA fragments were radioactively labeled by using a randomly primed DNA labeling kit (Roche Schweiz AG, Rotkreuz, Switzerland) in the presence of [α-^{32}P]dATP (Amersham Pharmacia Biotech, Little Chalfont, United Kingdom).

Northern analysis. For Northern analysis, either 1 (for probing with *hbpC*, *hbpA*, or *hbpD* gene fragments) or 8 μg (for probing with *hbpR* DNA) of RNA was denatured for 1 h at 50°C in the presence of 10 mM sodium phosphate buffer (pH 7.0)–50% DMSO–0.89 M glyoxylate in a total volume of 44.6 μl by standard procedures (4). After 0.1 volume of RNA loading buffer (50% sucrose, 15 mg of bromophenol blue)/ml was added, the glyoxylated RNA mixture was subsequently fractionated in a 1% agarose gel prepared in 10 mM sodium phosphate buffer (pH 7.0), with continuous buffer circulation. RNAs were transferred to Hybond-N membranes by blotting overnight in 10× SSC (1× SSC is 0.15 M NaCl plus 0.015 M sodium citrate).

The following *hbp* gene fragments were used as probes (Fig. 1B): for *hbpR*, a 0.89-kb *Ssp*I-*Nsi*I fragment from plasmid pHYBP111 (20); for *hbpC*, a 0.47-kb DNA fragment amplified in the PCR (for the location of the fragment, see Fig. 1B); for *hbpA*, a 0.74-kb *Hin*dIII-*Eco*RI fragment from plasmid pHBP160 (44); for *hbpD*, a 0.40-kb DNA fragment amplified by PCR.

Primer extension analysis. Primer extension reactions were carried out in 0.5-ml reaction tubes which were placed into a Crocodile II thermocycler (Appligene, Illkirch, France). First 2 pmol of primer (for *hbpC*, 5′-CGC AGG CCA AGA CTG ACA CCG G-3′, 122 bp downstream of the *hbpC* start codon; for *hbpD*, 5′-CCA CCA TGC AGC ATG ATC ACG G-3′, 122 bp downstream of the *hbpD* start codon) was mixed with 6 μg of total RNA in a total volume of 5 μl and covered with 1 drop of mineral oil (Sigma). Both primers were labeled at the 5′ end with fluorescent dye IRD-800 (MWG Biotech, Ebersberg, Germany). After an annealing step for 5 min at 68°C, the mixture was cooled to 42°C, and 3 μl of reverse transcriptase mixture was added. Final concentrations during the primer extension reaction were 50 mM Tris-HCl (pH 8.3), 50 mM NaCl, 8 mM $MgCl_2$, 1 mM dithiothreitol, 0.6 mM (each) deoxynucleotide (Amersham), 5% (vol/vol) DMSO, and 18 U of avian myeloblastosis virus reverse transcriptase (Amersham). After incubation for 1 h at 42°C the samples were denatured for 3 min at 95.5°C and loaded on a sequence gel next to samples from a sequence reaction performed on plasmid pHBP130 (44) with the same primers.

Construction of *luxAB*-based promoter-probe plasmids. A 704-bp DNA fragment containing the intergenic region between the *hbpR* and *hbpC* genes (region 1 in Fig. 1C) was obtained by PCR with *P. azelaica* HBP1 total DNA as described before (20). A 455-bp DNA fragment containing the intergenic region between the *hbpC* and *hbpA* genes (region 2 in Fig. 1C) and an 840-bp DNA fragment with the intergenic region between the *hbpA* and *hbpD* genes (region 3 in Fig. 1C) were obtained by PCR with *P. azelaica* HBP1 total DNA using primer pairs 5′-GCA TGC CAC TTG GGA GGT CAA GCG C-3′, 68 bp upstream of the *hbpC* stop codon, and 5′-TCT AGA CAT AGC GCC AGC CGG ACC-3′, 59 bp downstream of the *hbpA* start codon and 5′-GCA TGC GTA ACC GGT TGG TGA ACC-3′, 3 bp upstream of the *hbpA* stop codon, and 5′-TCT AGA TCC ATT CAA TGA GCC TGC C-3′, 3 bp downstream of the *hbpD* start codon, respectively. The cloning of the PCR-generated DNA fragments into pT7Blue(R) T vector (Novagen) resulted in plasmids pHYBP101 (region 2) and pHYBP102 (region 3). The inserts of plasmids pHYBP101 and pHYBP102 were sequenced and confirmed to be identical with the original *hbp* sequence. The inserts were then recovered as *Sph*I-*Xba*I fragments and ligated into *luxAB*-based promoter-probe vector pJAMA8 (20), as outlined in Fig. 1C. After transformation this resulted in plasmids pHYBP105 and pHYBP106, respectively. The *hbpC-hbpA* intergenic region of plasmid pHYBP105 was extended in plasmid pHYBP116 with a 0.24-kb upstream DNA region by exchanging the 0.16-kb *Sph*I-*Sal*I fragment of pHYBP105 for the 0.4-kb *Nar*I-*Sal*I fragment from plasmid pHBP130 (*Sph*I and *Nar*I were made blunt by treatment with T4 DNA polymerase) (Fig. 1C). By using the unique *Not*I sites at the flanks, all *luxAB* fusions were recovered and exchanged with the 3.2-kb *Not*I fragment present in Tn*5* delivery vector PCK218 (24). This resulted in plasmids pHYBP104 (P_{hbpC}-*luxAB*), pHYBP107 (region 2-*luxAB*), pHYBP108 (P_{hbpD}-*luxAB*), and pHYBP118 (region 4-*luxAB*).

Testing *hbp-lux* promoter-probe constructs in *E. coli*. All the different *hbp-lux* promoter-probe plasmids were cotransformed in *E. coli* with a plasmid expressing either the *hbpR* gene or an *hbpR* gene with an internal frameshift mutation (*hbpR*Δ). Plasmid pHYBP124 was obtained by cloning a 2.8-kb *Sal*I-*Nru*I DNA fragment from pHYBP122 (20), comprising the *hbpR* gene plus its own promoter, into pACYC184 (11) (digested with *Sal*I and *Nru*I). Plasmid pHYBP131 is similar to pHYBP124, except for having the *hbpR* gene inserted into the chloramphenicol resistance gene of pACYC184. Plasmid pHYBP125 (containing *hbpR*Δ) was created by first cloning a 2.8-kb *Not*I-*Xba*I fragment from pHYBP110 (20) into pUC28 (7) to give plasmid pHYBP123. Subsequently, the insert in pHYBP123 was retrieved as a 2.8-kb *Sal*I-*Nru*I fragment and cloned into pACYC184 (digested with *Sal*I and *Nru*I) to produce plasmid pHYBP125.

Single chromosomal insertion of *hbp-lux* promoter-probe constructs in *P. azelaica*. By using mini-Tn*5* delivery, the *hbp-lux* promoter-probe fusions of plasmids pHYBP104, pHYBP107, pHYBP108, and pHYBP118 were inserted into the chromosome of *P. azelaica*, as described previously (20). Selection for *P. azelaica* exconjugants was done on MM plates with 50 μg of kanamycin/ml and 2.9 mM 2-HBP. Proper insertion of the constructs was verified by Southern hybridization of the *P. azelaica* exconjugants (data not shown).

In *P. azelaica* HBP108 (containing the *hbpD′*::*lux* fusion) the *hbpR* gene was disrupted by single recombination as described earlier (20). Obtained *P. azelaica* HBP108 recombinants were checked for proper disruption of the *hbpR* gene by PCR and Southern hybridizations (the resulting strain is referred to as HBP108121; Table 1).

Enzyme assays. Induction experiments with *luxAB*-harboring *E. coli* and *P. azelaica* strains were performed by in MM at 30°C as described before (20). Expression of luciferase was analyzed by measuring bioluminescence on whole

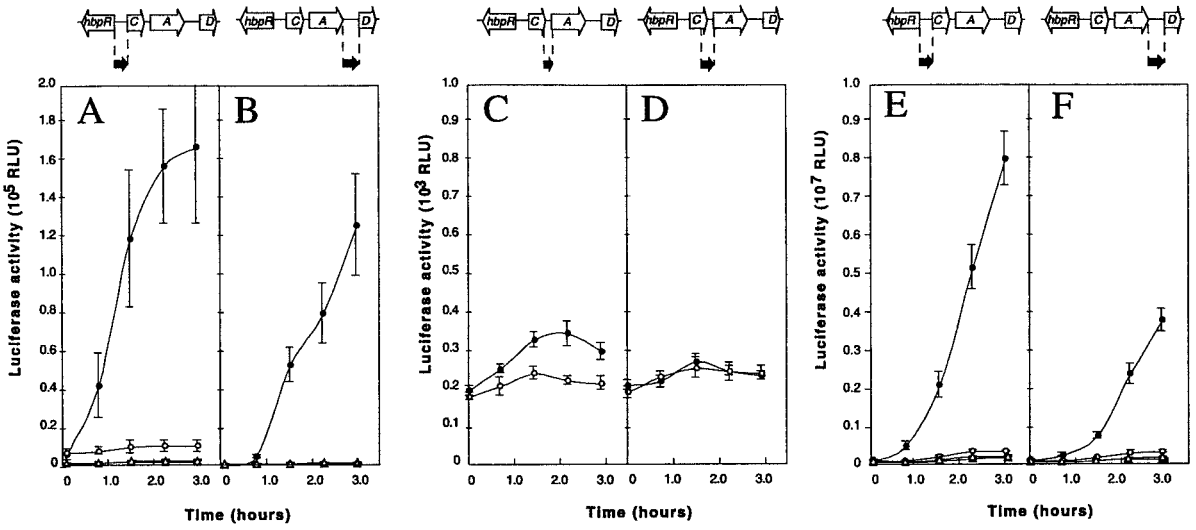

FIG. 2. Promoter activity from *hbp*-derived intergenic regions 1 to 4 (Fig. 1) in *P. azelaica* (A to D) and *E. coli* (E and F), with a functional *hbpR* (circles) or with a disrupted *hbpR* (triangles). Experiments were carried out with 0.2 mM 2-HBP (solid symbols) or with DMSO only (open symbols). (A) *P. azelaica* HBP104 (*hbpC′*::*luxAB*) and HBP104121 (HBP104 with disrupted *hbpR*). (B) *P. azelaica* HBP108 (*hbpD′*::*luxAB*) and HBP108121 (HBP108 with disrupted *hbpR*). (C) *P. azelaica* HBP107 (*hbpA′*::*luxAB*). (D) *P. azelaica* HBP118 (*hbpC-A′*::*luxAB*). (E) *E. coli* DH5α with pHYBP103 (*hbpC′*::*luxAB*) plus pHYBP124 (intact *hbpR*) or with pHYBP103 plus pHYBP125 (disrupted *hbpR*). (F) *E. coli* DH5α with pHYBP106 (*hbpD′*::*luxAB*) plus pHYBP124 or with pHYBP106 plus pHYBP125. Solid arrows, positions and orientations of the intergenic regions with respect to the *luxAB* fusion. Note that the scale of luciferase activity in panels A and B is different from that in panels C to F. Error bars, standard deviations in two independent experiments each carried out in triplicate. RLU, relative light units.

cells at a final *n*-decanal concentration of 2 mM in a MicroLumat LB 96 P luminometer (Berthold AG, Regensdorf, Switzerland) as described previously (47).

Activities of the HbpA, HbpC, and HbpD enzymes were measured in cell extracts prepared from 3-ml samples taken from chemostat-grown cultures of *P. azelaica* HBP1. Preparation of cell extract and enzyme assays for 2-hydroxybiphenyl-3-monooxygenase (HbpA), 2,3-dihydroxybiphenyl dioxygenase (HbpC), and 2-hydroxy-6-oxo-6-phenyl-2,4-dienoic acid hydrolase (HbpD) were carried out as described previously (20).

HPLC analysis. The disappearance of 2-HBP and the formation of 2-HBP intermediates during induction of chemostat-grown cells of *P. azelaica* HBP1 with 0.5 mM 2-HBP were determined by high-pressure liquid chromatography (HPLC) analysis with a Gynkotek (Germering, Germany) HPLC system. The system consisted of a Gina 50 automated-injection module, a M480 G gradient pump, an on-line degasser, and a UVD 340 S photodiode array detector. The column used was a Nucleosil 100-5 C_{18} reversed-phase column. The mobile phase was prepared by mixing 65% of solution A (containing 10 mM H_3PO_4 at pH 3.0 in water) and 35% of solution B (which is 90% [vol/vol] methanol and 10% solution A). The flow rate was 0.6 ml/min. Samples were taken from the chemostat culture, cells were spun down by centrifugation, and the supernatant was acidified and stored at −20°C. Immediately before HPLC injection the supernatants were filtered through 0.2-μm-pore-size filters to remove cell debris.

RESULTS

Expression of the *hbpCAD* genes is mediated from two separate promoters. Since the *hbpC*, *hbpA*, and *hbpD* genes displayed rather abnormally large intergenic regions (Fig. 1B), we investigated whether all three genes would be expressed from one promoter or from more. To identify possible promoters for *hbpCAD* expression, transcriptional fusions between different *hbp* intergenic regions (Fig. 1C, regions 1 to 4) and the *luxAB* genes of *Vibrio harveyi* were constructed. These fusions were then placed randomly into the chromosome of *P. azelaica* HBP1 by mini-Tn*5* transposition. Southern analysis confirmed that all strains had acquired the transcriptional fusions by a proper transposition and not by homologous recombination of the complete Tn*5*-bearing plasmids at the *hbp* locus (data not shown).

After induction with 2-HBP for 3 h, *P. azelaica* strain HBP104 (carrying the *hbpC′*::*luxAB* fusion) showed a 17-fold increase in bioluminescence compared to that for uninduced conditions (Fig. 2A). This confirmed our previous results that a promoter activated by HbpR was located upstream of *hbpC* (20). In contrast, strain HBP107 (*hbpA′*::*luxAB*) showed only a slight increase in bioluminescence activity 3 h after the addition of 2-HBP; this corresponds to a maximum induction factor of 1.6 (Fig. 2C). Furthermore, absolute luminescence activities of strain HBP107 were 45-fold lower than those of strain HBP104. From this we concluded that no, or at most a very weak, promoter was present in the region between *hbpC* and *hbpA*. To make sure that no additional promoters, activated in the presence of 2-HBP, were located further upstream, the *hbpC-hbpA* intergenic region was extended to include 0.3 kb of the 3′ part of the *hbpC* gene (Fig. 1C, region 4). A *P. azelaica* strain with this *hbpC-hbpA′*::*luxAB* fusion (HBP118) displayed basically the same bioluminescence levels as strain HBP107, and no induction with 2-HBP was detected (Fig. 2D). The next region we examined, i.e., the region upstream of *hbpD*, again showed promoter activity (Fig. 2B). Luciferase activity after 3 h of induction with 2-HBP was 75% of that observed with the *hbpC′*::*luxAB* fusion (Fig. 2A).

In derivatives of *P. azelaica* strains HBP104 (*hbpC′*::*luxAB*) and HBP108 (*hbpD′*::*luxAB*) in which the *hbpR* gene was disrupted by homologous recombination, no induction of luciferase activity in the presence of 2-HBP was measurable (Fig. 2A and B). This indicated that expression of not only *hbpC*, as previously reported (20), but also *hbpD* was controlled by HbpR.

Interestingly, the induction of luciferase activity from the

hbpD promoter showed a distinct lag, whereas that from the *hbpC* promoter started almost immediately after 2-HBP was added to the cells (Fig. 2A and B). For both promoter constructs we observed a maximal luciferase activity, which for P_{hbpC} occurred at 2-HBP concentrations around 0.5 mM but which for P_{hbpD} occurred at 2 mM 2-HBP. However, at higher 2-HBP concentrations, responses from both promoters decreased sharply. This might be caused either by a direct down regulation of the promoter response or by general toxic effects of 2-HBP or its metabolite 2,3-dihydroxybiphenyl on cellular metabolism or on the luciferase system itself (30, 50).

To exclude the possibility that the role of HbpR in activating transcription from two promoters upstream of *hbpC* and *hbpD* was indirect, we repeated the induction studies with *E. coli* containing a plasmid with *hbpC′*::*luxAB* or with *hbpD′*::*luxAB* plus a compatible plasmid with *hbpR* (pHYBP124). Luciferase activity was induced with 2-HBP from both *hbpC′*::*luxAB* and from *hbpD′*::*luxAB* in *E. coli* (Fig. 2E and F). This confirmed the direct role of HbpR in transcriptional activation from P_{hbpC} and P_{hbpD}. In contrast, a plasmid with *hbpA′*::*luxAB* did not show 2-HBP-dependent light emission in *E. coli* (not shown). When a plasmid with a frameshift in the open reading frame of *hbpR* was provided (pHYBP125) instead of a functional *hbpR*, none of the *hbp*::*luxAB* transcriptional fusions led to 2-HBP-dependent light emission in *E. coli*. In cells without functional HbpR, addition of 2-HBP even reduced background bioluminescence levels by 20 (from P_{hbpC}) and 31% (from P_{hbpD}).

Two separate transcripts are formed from the *hbpCAD* genes. The lengths of transcripts that appeared upon the induction of the *hbpCAD* genes were estimated by Northern analysis with RNA isolated from a chemostat culture of wild-type strain HBP1 just before and after a shift to medium with 0.5 mM 2-HBP. For each of the *hbp* structural genes, transcripts were detectable only after induction with 2-HBP (Fig. 3). No apparent differences in the time of appearance of the *hbp* mRNAs, except that of *hbpR*, were detectable on Northern hybridization. Within 7 min after the induction start, *hbpC*-specific transcripts appeared, with estimated lengths of 1.0 and 3.2 kb (Fig. 3A). The longer (3.2-kb) transcript was also visible on blots hybridized with the *hbpA* probe. In addition, blots hybridized with a *hbpA* gene fragment showed a smaller, 1.9-kb transcript (Fig. 3B). Two clear *hbpD*-specific transcripts with estimated sizes of 0.9 and 1.7 kb were detected (Fig. 3C). RNA isolated only 3 min after induction with 2-HBP showed transcripts which were still incomplete. For example, the *hbpCA* transcript had a size of around 2.5 kb after 3 min (Fig. 3A and B). This demonstrated that the 1.0-kb transcript seen in Fig. 3A after 3 min encompasses *hbpC*, whereas the 1.9-kb transcript containing *hbpA* only cannot be seen yet, since it has to be formed from the complete 3.2-kb *hbpCA* transcript. In contrast, hybridization with the *hbpR* probe resulted in a 1.8-kb transcript, which was visible both before and after the shift, although the band intensities increased about twofold after induction with 2-HBP (Fig. 3D).

P_{hbpC} and P_{hbpD} are σ^{54}-dependent promoters. The in vivo transcriptional start sites of the *hbpC* and *hbpD* genes in *P. azelaica* HBP1 were determined by primer extension analysis with RNA isolated from a chemostat culture of strain HBP1 7 min after induction with 0.5 mM 2-HBP. A clear extension product

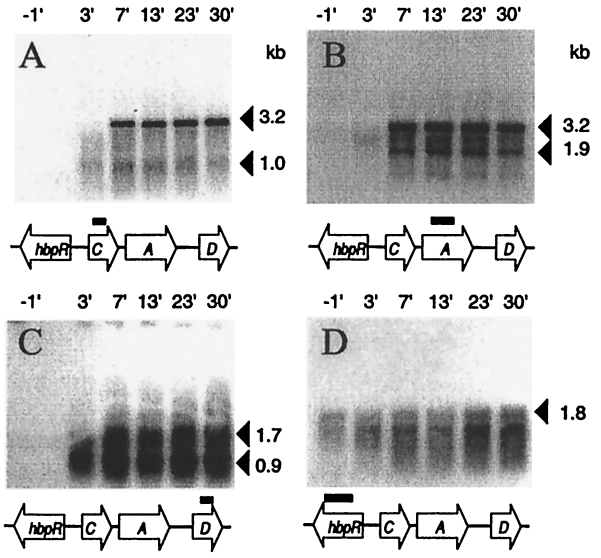

FIG. 3. Northern analysis of the different *hbp* transcripts. RNA was isolated from a carbon-limited glucose-grown chemostat culture of *P. azelaica* HBP1, 1 min before and 3, 7, 13, 23, and 30 min after a shift to an immediate pulse of 0.5 mM 2-HBP and subsequent medium change to glucose plus 0.5 mM 2-HBP. From each sample, approximately 1 (A to C) or 8 μg (D) of RNA was blotted in each lane and hybridized with radioactively labeled probes against *hbpC* (A), *hbpA* (B), *hbpD* (C), or *hbpR* (D). Black bars, locations and sizes of the gene-specific probes. Transcript sizes are marked on the right. The presence of two bands in panel D is an artifact caused by the abundance of 16S rRNA migrating slightly below the *hbpR* transcript.

could be seen for the *hbpC* gene after induction with 2-HBP; this product was not visible under uninduced conditions (Fig. 4A). This transcript corresponded to a transcriptional start site 68 bp upstream of the ATG start codon of the *hbpC* gene (Fig. 5A). For the *hbpD* gene, a specific cDNA was detected after 2-HBP induction; the cDNA corresponded to a transcriptional start site 133 bp upstream of the ATG start codon of the *hbpD* gene (Fig. 4B and 5B). This confirmed that the regions upstream of *hbpC* and *hbpD* contained a promoter activated in the presence of 2-HBP. Upstream of the transcriptional start sites of the *hbpC* and *hbpD* genes, −24 (GG)/−12 (GC) motifs, which are typical for σ^{54}-dependent promoters, were found (Fig. 4 and 5).

To establish if RNAP-σ^{54} was indeed involved in the transcriptional activation from P_{hbpC} and P_{hbpD}, induction experiments were carried out with *E. coli* strains devoid of the *rpoN* gene (i.e., *E. coli* ET8045). No induction was detected in *E. coli* ET8045 harboring plasmids pHYBP124 (with *hbpR*) and pHYBP103 (with *hbpC′*::*luxAB*) or plasmids pHYBP124 and pHYBP106 (with *hbpD′*::*luxAB*), whereas luciferase activity increased as expected after exposure of *E. coli* ET8000 to 2-HBP (Table 2). This indicated that RNAP-σ^{54} is the holoenzyme which is responsible for transcription from the P_{hbpC} and P_{hbpD} promoters.

IHF is required for transcription from P_{hbpC} and P_{hbpD}. To study if additional factors were needed for transcriptional activation from P_{hbpC} and P_{hbpD}, we carried out similar induction experiments with *E. coli* strains lacking the structural genes for HU or for IHF (Table 3). In the absence of IHF, the observed induction factors obtained for the expression from P_{hbpC} (1.2)

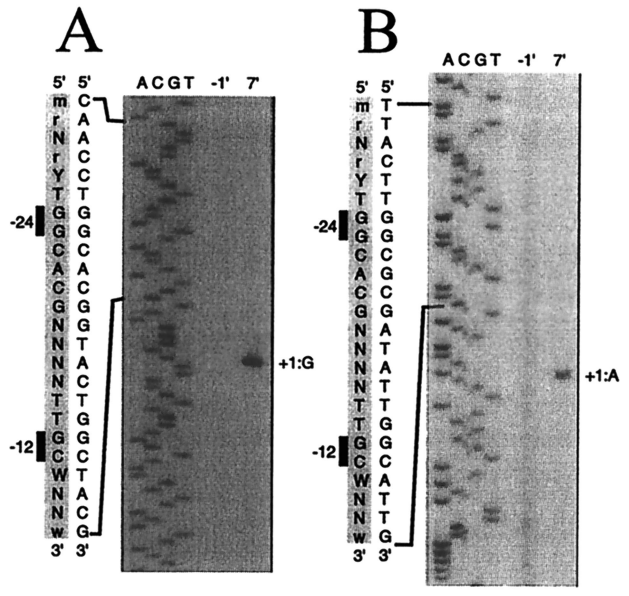

FIG. 4. Mapping of the in vivo transcriptional start sites of the *hbpC* (A) and the *hbpD* (B) genes by primer extension analysis of RNA isolated from a glucose-grown chemostat culture of *P. azelaica* HBP1 1 min before and 7 min after induction with 0.5 mM 2-HBP. The primer extension products were run next to products of sequence reactions performed with the same primer. +1, transcriptional start site. An expanded view of the (complementary) nucleotide sequence (5′-to-3′ direction) surrounding the σ^{54}-dependent promoter is shown at the left of the panels. Also shown is an alignment with a consensus sequence for −24/−12 promoters (R = A or G; Y = C or T; M = A or C; W = A or T; N = any nucleotide) (5).

and P_{hbpD} (0.96) were much lower than those in the presence of IHF (ratios of 20 and 2.9, respectively). This indicated that transcription from P_{hbpC} and P_{hbpD} upon induction with 2-HBP was restricted in the absence of IHF. Without HU, expression from P_{hbpC} in the presence of 2-HBP was fourfold lower than with HU but the obtained induction factors were virtually the same (21 without HU and 20 with HU). Hence, transcription from P_{hbpC} seemed not to be affected by the absence of HU. 2-HBP-induced expression from P_{hbpD} in an HU-negative background, however, decreased ninefold compared to that in a wild-type background. The observed induction factor was reduced about twofold (from 2.9 to 1.5) in an HU-negative background.

Induction dynamics of the 2-HBP pathway. In order to determine the effectiveness of the overall induction of the 2-HBP pathway, we induced chemostat-grown cells of *P. azelaica* HBP1 with 2-HBP and analyzed changes in mRNA abundance, in specific enzyme activities of the 2-HBP pathway, and in metabolites during the first 4 h after induction. Steady-state cultures grown under carbon limitation with glucose displayed only basal levels of activity of the three 2-HBP-specific enzymes. After addition of 2-HBP to the chemostat to achieve an immediate concentration of 0.5 mM (and, therefore, a temporary release of carbon limitation), we observed a very fast formation of specific mRNAs for *hbpCA* and *hbpD* (Fig. 3). After approximately 1.5 h, the mRNA levels decreased to much lower levels (not shown). Specific activities of HbpC, HbpA, and HbpD started to increase from about 5 min after induction (Fig. 6). HbpC activity peaked after around 30 min at a maximum of 250 mU/mg of protein and then rapidly decreased. This decrease could be partially caused by reactions which irreversibly inhibited the enzyme (23). Activities increased much more steadily for HbpA and HbpD and did not decrease during the first 4 h after induction (Fig. 6A).

After a short lag of about 30 min, 2-HBP started to disappear from the chemostat (Fig. 6B). The product of the first reaction, 2,3-dihydroxybiphenyl, which is formed by HbpA, could not be detected in the chemostat, probably because of very rapid conversion by an excess of HbpC enzyme. Transient accumulation of the *meta* cleavage product (inset of Fig. 6B) occurred, indicating that for a short time period hydrolysis of the *meta* cleavage product was rate limiting. Also, a temporary accumulation of benzoate, which is one of the products of the reaction catalyzed by HbpD, was measured. This indicated that the enzymes for the conversion of benzoate were absent during growth without 2-HBP. After 2 h, neither substrate nor intermediates could be detected in the supernatant of the continuous culture, even though 2-HBP was continuously supplied with the fresh medium.

DISCUSSION

Previously, we had determined that the HbpR protein, which is encoded by a 1,710-bp large open reading frame closely linked and oriented oppositely to the *hbpCAD* genes, is the main transcriptional activator of the 2-HBP pathway (20). As we now discovered, HbpR actually activates transcription from two separate promoters in this gene cluster. One of these (P_{hbpC}) is located upstream of the *hbpC* gene, whereas the other one appears to be located upstream of the *hbpD* gene (P_{hbpD}). Our evidence that HbpR is activating expression from both promoters in the *hbp* cluster is the following. Disruption of the *hbpR* gene in *P. azelaica* strains containing either a *hbpC′*::*luxAB* or a *hbpD′*::*luxAB*fusion integrated in monocopy on the chromosome led to complete abolishment of luciferase expression in the presence of 2-HBP. Furthermore, we could show that the presence of an intact *hbpR* was required in *E. coli* to activate transcription from both *hbpC* and the *hbpD* promoter. In contrast to what was found for the regions upstream of the *hbpC* and *hbpD* genes, no promoter regulated by HbpR could be identified upstream of the *hbpA* gene.

The synthesis of different transcripts for the *hbpCAD* genes, originating from P_{hbpC} and P_{hbpD} upon induction with 2-HBP, was confirmed by Northern analysis. Transcripts encompassed either *hbpC* and *hbpA* (3.2 kb), as expected when starting from P_{hbpC}, or *hbpD* alone (1.7 kb), when transcribed from P_{hbpD}. Northern analysis also suggested that an effective cleavage or processing of the 3.2-kb *hbpCA* mRNA took place between *hbpC* and *hbpA*, resulting in the formation of an *hbpC*-specific (1.0-kb) and an *hbpA*-specific (1.9-kb) transcript. The occurrence of an *hbpA*-specific transcript of 1.9 kb and the absence of a specific promoter directly in front of *hbpA* are evidence against the possibility that a weak terminator would be present directly downstream of *hbpC*. The smaller 0.9-kb *hbpD*-specific transcript, which was observable in Northern hybridizations, might have been generated from early termination at a 27-bp-long ρ-independent terminator structure 21 bp downstream of the *hbpD* gene (Fig. 1D). A transcript comprising all three *hbpCAD* genes was not found, although some material of

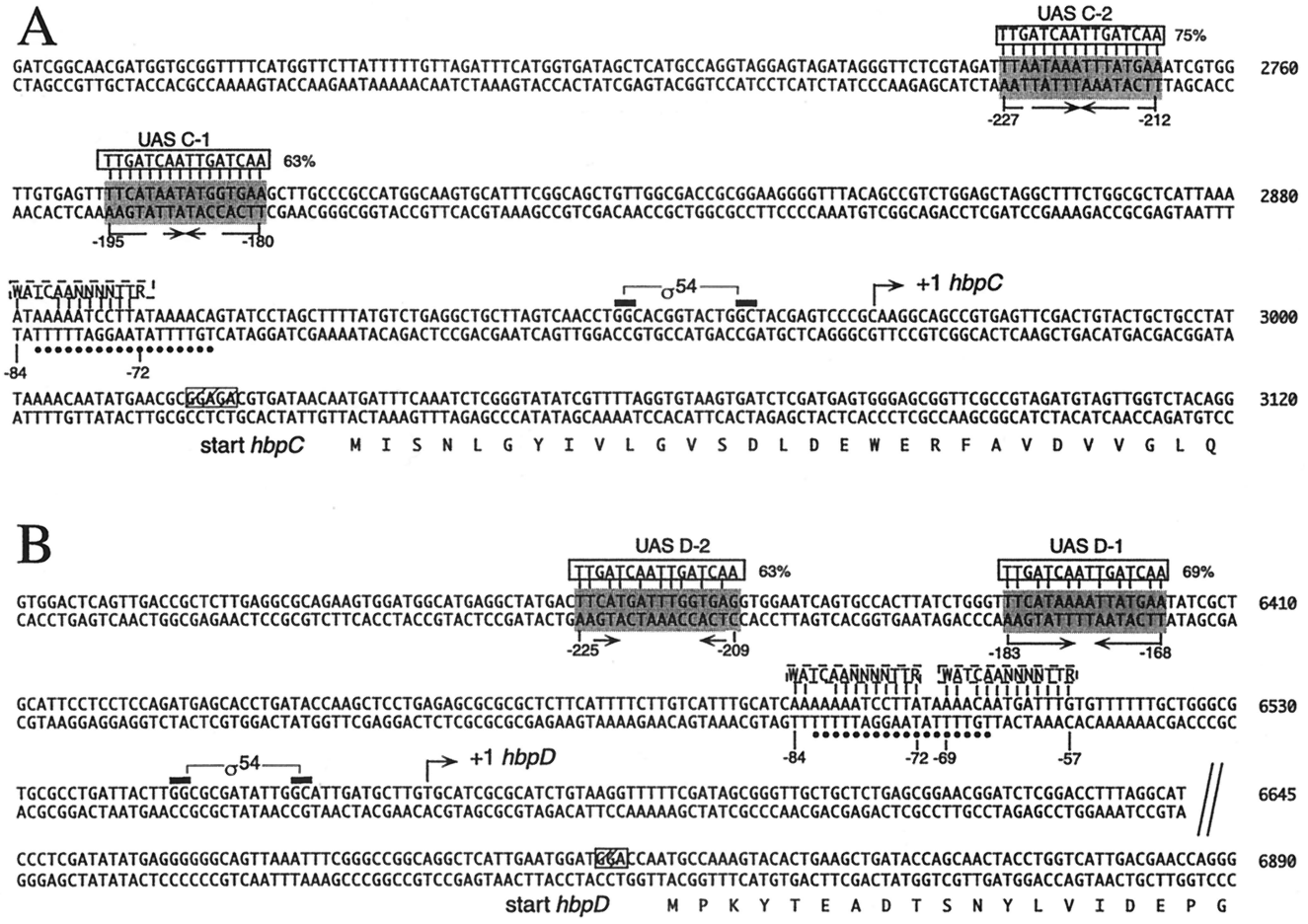

FIG. 5. Sequences of the DNA regions upstream of the *hbpC* (A) and the *hbpD* (B) genes. The base pair numbering corresponds to that of the GenBank entry under accession no. U73900. Bent arrows, transcriptional start sites (+1) for the *hbpC* and *hbpD* genes and the direction of transcription; black bars, −24 and −12 elements in σ^{54}-dependent promoters P_{hbpC} and P_{hbpD}; shaded boxes, putative UASs for HbpR binding (arrows underneath, palindromic structures within these DNA regions). Alignments with the consensus sequence for XylR/DmpR-type UASs (5′-TTGATCAATTGATCAA-3′; solid boxes) as proposed by Pérez-Martín and de Lorenzo (36) are shown at the top of putative UASs with numbers indicating the percentages of identity between the two DNA motifs. Dashed boxes, alignments of DNA regions similar to the consensus IHF binding site (5′-WATCAANNNNTTR-3′, where W = A or T, R = A or G, and N = any nucleotide) (15); dots, 18-bp-long DNA stretch overlapping the putative IHF sites and in common to both the *hbpC* and the *hbpD* promoters. The numbers below putative UASs and IHF sites indicate the relative positions with respect to the transcriptional start site. The N-terminal parts of HbpC and HbpD are indicated below the corresponding sequences. Hatched boxes, putative ribosome binding sites.

larger size weakly hybridized with either the *hbpC*, *hbpA*, or *hbpD* probe (Fig. 3). This indicates that a transcription terminator must be present downstream of the *hbpA* gene. The DNA sequence in this region showed a 30-bp-long inverted repeat 45 bp downstream of the *hbpA* gene, which might function as a ρ-independent terminator (Fig. 1D).

Activation of both the *hbpC* and the *hbpD* promoters was dependent on alternative sigma factor σ^{54}. This became evi-

TABLE 2. Activation from P_{hbpC} and P_{hbpD} in dependency of σ^{54}

Strain	Plasmids[d]	Luciferase activity (relative light units) ± SD[a] with:		Induction factor[c]
		No inducer	2-HBP[b]	
ET8000	pHYBP103, pHYBP124	7.48E+04 ± 1.27E+04	1.49E+06 ± 2.21E+05	20
	pHYBP106, pHYBP124	1.89E+05 ± 9.49E+03	1.34E+06 ± 1.26E+05	7.1
ET8045[e]	pHYBP103, pHYBP124	8.50E+04 ± 5.00E+03	8.11E+04 ± 7.94E+03	0.95
	pHYBP106, pHYBP124	2.39E+05 ± 1.57E+04	2.49E+05 ± 1.02E+04	1.1

[a] All values were obtained in two independent experiments, each performed in triplicate.
[b] Assay concentration for 2-HBP was 0.2 mM.
[c] Induction factor is the quotient of the bioluminescence measured with and without the inducer.
[d] pHYBP103 contains *hbpC*::*luxAB*; pHYBP106 contains *hbpD*::*luxAB*; pHYBP124 contains *hbpR*.
[e] RpoN mutant.

TABLE 3. Activation from P_{hbpC} and P_{hbpD} in dependency of IHF and HU

Strain[d]	Plasmids[e]	Luciferase activity (relative light units) ± SD[a] with:		Induction factor[c]
		No inducer	2-HBP[b]	
N99	pHYBP103, pHYBP131	1.08E+05 ± 7.70E+03	2.13E+06 ± 5.06E+05	20
	pHYBP106, pHYBP131	1.26E+05 ± 1.53E+04	3.72E+05 ± 4.95E+04	2.9
A5475	pHYBP103, pHYBP131	6.22E+04 ± 9.73E+03	7.21E+04 ± 1.49E+04	1.2
	pHYBP106, pHYBP131	5.18E+04 ± 1.26E+04	4.96E+04 ± 1.71E+04	0.96
A5196	pHYBP103, pHYBP131	2.61E+04 ± 1.34E+03	5.56E+05 ± 4.88E+04	21
	pHYBP106, pHYBP131	2.74E+04 ± 3.80E+03	4.06E+04 ± 4.54E+03	1.5

[a] All values were obtained in two independent experiments, each performed in triplicate.
[b] Assay concentration for 2-HBP was 0.2 mM.
[c] Induction factor is the ratio of the bioluminescence measured with and without the inducer.
[d] *E. coli* strains A5196 and A5475 are derivatives of *E. coli* N99 without HU protein and IHF, respectively.
[e] Plasmid pHYBP103 contains *hbpC*::*luxAB*, pHYBP106 contains *hbpD*::*luxAB*, and pHYBP131 contains *hbpR*.

dent from mapping the transcriptional start sites of the *hbpCA* and *hbpD* transcripts and by studying expression of both promoters in *E. coli* mutants lacking the σ^{54} subunit. This is in line with other pathways regulated by XylR/DmpR subclass members, such as AphR (2), DmpR (46), MopR (43), TbuT (9), TouR (3), and XylR (reviewed in reference 39). In addition to the σ^{54} factor, IHF was found to be important for optimal transcriptional activation from P_{hbpC} and P_{hbpD} in *E. coli*. Examination of the DNA sequence upstream of P_{hbpC} and P_{hbpD} revealed one and two regions, respectively, with significant homology to the consensus IHF-binding site (15) (Fig. 5). These putative IHF-binding sites are centered on an 18-bp-long DNA stretch common to both promoters. IHF was also needed for maximum expression from the XylR-responsive P_u promoter (1, 35, 37) and for optimum in vivo expression from the DmpR-regulatable P_o promoter (49). Other consensus sequence features between the *hbpC* and the *hbpD* promoters point to possible binding sites for HbpR (Fig. 5). The base pairs of these two 16-bp regions are between 63 and 75% identical to those of the consensus binding site for XylR/DmpR (36).

It was surprising to find that luciferase expression from the P_{hbpD} promoter occurred significantly later than that from the P_{hbpC} promoter when tested both in *P. azelaica* and in *E. coli* (Fig. 2). However, since mRNA for *hbpD* was not being formed any later than *hbpC* mRNA in *P. azelaica* HBP1 upon

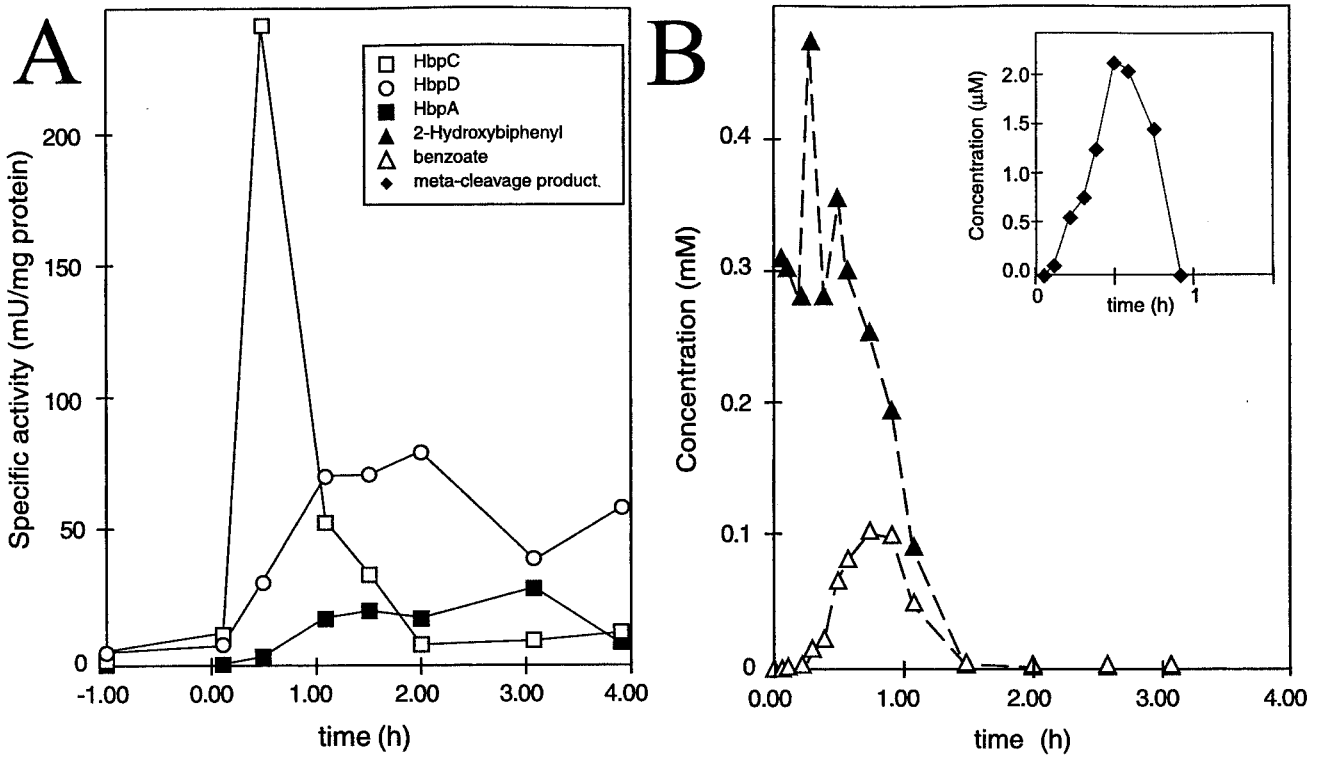

FIG. 6. Temporary changes in enzyme activities of the HBP pathway (A) and in concentrations of 2-HBP and its intermediates (B) upon induction of a glucose-grown steady-state continuous culture of *P. azelaica* with 2-HBP. Time zero is the time of addition of 2-HBP to the culture. (By inset) Concentrations of 2-hydroxy-6-oxo-6-phenyl-2,4-hexadienoic acid, the *meta* cleavage product. Only very low concentrations of this compound could be measured (note the difference in scale). The *meta* cleavage product, however, is unstable in solution at pH 7 (22).

induction (Fig. 3), we must assume that the slower induction of luciferase activity from the P_{hbpD} promoter is a translational effect. Luciferase expression from P_{hbpD} was also lower than that from P_{hbpC} (after the same induction time and with the same 2-HBP concentration). Although it is known that the luciferase gene may alter the promoter configuration (14), a comparison of the amounts of specific mRNA formed suggested that less *hbpD* mRNA than *hbpCA* mRNA was synthesized upon induction with 2-HBP (not shown). This may point to a suboptimal local geometry of the P_{hbpD} promoter and explain why we found a weak but evident coassisting role of HU in the activation from P_{hbpD} (Table 3). Aberrant spacing of the two HbpR binding sites at the P_{hbpD} promoter might be responsible for this. From extensive work on the XylR regulator protein and its activation of the P_u promoter in *Pseudomonas putida*, it is known that the spacing and orientation of the two XylR-binding sites are very important for expression of P_u. Optimal expression is obtained only when both sites are oriented on the same side of the DNA helix (1, 36). The centers of the two XylR binding sites in the P_u and P_s promoters and of the DmpR binding sites in the P_o promoter are separated by three complete DNA helical turns (36). For the P_{hbpC} promoter three helical turns (assuming one DNA helical turn corresponds to 10.5 nucleotides) separated the centers of the putative HbpR-binding sites (Fig. 5B). However, the spacing for the putative HbpR-binding sites in the P_{hbpD} promoter was four helical turns. In addition, the HbpR-binding sites at the P_{hbpD} promoter seem rotated by 51° (when assuming no bends in the DNA) with respect to the −12/−24 region.

The *hbpCA* and *hbpD* genes of *P. azelaica* HBP1 are organized unusually for a catabolic gene cluster regulated by an XylR/DmpR-type activator protein (51). Only three structural genes make up the cluster, and these genes have rather large intergenic distances (315 bp between *hbpC* and *hbpA* and 831 bp between *hbpA* and *hbpD*). This may point to a relatively recent insertion of a DNA fragment containing the *hbpA* gene into an ancestor cluster with the *hbpC* and *hbpD* genes. Newly arranged gene clusters are interesting to study, since they may show peculiarities in the organization of transcription and particular adaptive features ensuring proper expression of the complete pathway. For the 2-HBP pathway, one of the most important tasks is to prevent the substances 2-HBP and its intermediates from becoming toxic to the cell. Both 2,3-dihydroxybiphenyl and the *meta* cleavage product of 2,3-dihydroxybiphenyl are product inhibitors for enzymatic activities of HbpA (48) and HbpC (23), respectively. Furthermore, 2,3-dihydroxybiphenyl may auto-oxidize to quinones which interfere with the electron transport chain (19, 50). Several features of the *hbp* transcriptional organization seem to be responsible for accomplishing proper induction of the 2-HBP pathway and preventing buildup of toxic intermediates. For example, the activity of HbpA (2-HBP monooxygenase) is kept low compared to that of HbpC (the extradiol dioxygenase) (20) and HbpC activity appears much faster than HbpA or HbpD activity (Fig. 6). Therefore, no accumulation of 2,3-dihydroxybiphenyl is seen in a continuous culture pulsed with 2-HBP. By having *hbpC* transcribed first and possibly by processing the *hbpCA* transcript, cells ensure that HbpC is synthesized faster than HbpA.

If at any point during evolution a fragment containing *hbpA* became inserted into a gene cluster with *hbpC* and *hbpD*, this would have disrupted proper transcription of *hbpD*, since a transcription terminator seems to be present downstream of *hbpA*. This might be the reason for the presence of a second separate promoter in front of *hbpD*, which ensures that transcription of *hbpD* starts simultaneously with that of *hbpC*. However, since translation of the *hbpD* mRNA seems less effective, the *meta* cleavage product of 2,3-dihydroxybiphenyl can accumulate rapidly. This appears to be the one feature which is not "smoothly" controlled by the cells, since the *meta* cleavage product can irreversibly inhibit activity of the HbpC extradiol dioxygenase (23). Therefore, fast and intensive transcription of *hbpC* serves two purposes, i.e., lowering the concentration of toxic 2,3-dihydroxybiphenyl and replenishing the inactivated enzyme.

ACKNOWLEDGMENTS

We thank V. de Lorenzo (Centro Nacional de Biotecnologia, CSIC, Madrid, Spain) for kindly supplying us plasmid pCK218 and strains N99, A5196, and A5475. Further we thank R. Dixon (Nitrogen Fixation Laboratory, John Innes Centre, Norwich, United Kingdom) for providing us with strains ET8000 and ET8045. The help of Christoph Werlen with the chemostat cultivations is gratefully acknowledged.

The work of M.C.M.J. was supported by grant 5001-044754 from the Swiss Priority Program Environment.

REFERENCES

1. **Abril, M.-A., M. Buck, and J. L. Ramos.** 1991. Activation of the *Pseudomonas* TOL plasmid upper pathway operon. J. Biol. Chem. **266:**15832–15838.
2. **Arai, H., S. Akahira, T. Ohishi, M. Maeda, and T. Kudo.** 1998. Adaptation of *Comamonas testosteroni* TA441 to utilize phenol: organization and regulation of the genes involved in phenol degradation. Microbiology **144:**2895–2903.
3. **Arenghi, F. L., M. Pinti, E. Galli, and P. Barbieri.** 1999. Identification of the *Pseudomonas stutzeri* OX1 toluene-*o*-xylene monooxygenase regulatory gene (*touR*) and of its cognate promoter. Appl. Environ. Microbiol. **65:**4057–4063.
4. **Ausubel, F. M., R. Brent, R. E. Kingston, D. D. Moore, J. G. Seidman, J. A. Smith, and K. Struhl (ed.).** 1996. Current protocols in molecular biology. John Wiley & Sons, Inc., New York, N.Y.
5. **Barrios, H., B. Valderrama, and E. Morett.** 1999. Compilation and analysis of σ^{54}-dependent promoter sequences. Nucleic Acids Res. **27:**4305–4313.
6. **Baumann, B., M. Snozzi, A. J. B. Zehnder, and J. R. van der Meer.** 1996. Dynamics of denitrification activity of *Paracoccus denitrificans* in continuous culture during aerobic-anaerobic changes. J. Bacteriol. **178:**4367–4374.
7. **Benes, V., Z. Hostomsky, L. Arnold, and V. Paces.** 1993. M13 and pUC vectors with new unique restriction sites for cloning. Gene **130:**151–152.
8. **Bertoni, G., N. Fujita, A. Ishihama, and V. de Lorenzo.** 1998. Active recruitment of σ^{54}-RNA polymerase to the *Pu* promoter of *Pseudomonas putida*: role of IHF and αCTD. EMBO J. **17:**5120–5128.
9. **Byrne, A. M., and R. H. Olsen.** 1996. Cascade regulation of the toluene-3-monooxygenase operon (*tbuA1UBVA2C*) of *Burkholderia pickettii* PKO1: role of the *tbuA1* promoter (*PtbuA1*) in the expression of its cognate activator, TbuT. J. Bacteriol. **178:**6327–6337.
10. **Carmona, M., V. de Lorenzo, and G. Bertoni.** 1999. Recruitment of RNA polymerase is a rate-limiting step for the activation of the σ^{54} promoter *Pu* of *Pseudomonas putida*. J. Biol. Chem. **274:**33790–33794.
11. **Chang, A. C. Y., and S. N. Cohen.** 1978. Construction and characterization of amplifiable multicopy DNA cloning vehicles derived from the P15A cryptic miniplasmid. J. Bacteriol. **134:**1141–1156.
12. **de Lorenzo, V., M. Herrero, M. Metzke, and K. N. Timmis.** 1991. An upstream XylR- and IHF-induced nucleoprotein complex regulates the σ^{54}-dependent Pu promoter of TOL plasmid. EMBO J. **10:**1159–1167.
13. **Fernández, S., V. de Lorenzo, and J. Pérez-Martín.** 1995. Activation of the transcriptional regulator XylR of *Pseudomonas putida* by release of repression between functional domains. Mol. Microbiol. **16:**205–213.
14. **Forsberg, Å. J., G. D. Pavitt, and C. F. Higgins.** 1994. Use of transcriptional fusions to monitor gene expression: a cautionary tale. J. Bacteriol. **176:**2128–2132.
15. **Friedman, D. I.** 1988. Integration host factor: a protein for all reasons. Cell **55:**545–554.
16. **Gerhardt, P., R. G. E. Murray, R. N. Costilow, E. W. Nester, W. A. Wood, N. R. Krieg, and G. B. Phillips (ed.).** 1981. Manual of methods for general bacteriology. American Society for Microbiology, Washington, D.C.
17. **Herrero, M., V. de Lorenzo, and K. N. Timmis.** 1990. Transposon vectors

containing non-antibiotic resistance selection markers for cloning and stable chromosomal insertion of foreign genes in gram-negative bacteria. J. Bacteriol. **172:**6557–6567.
18. **Hoover, T. R., E. Santero, S. Porter, and S. Kustu.** 1990. The integration host factor stimulates interaction of RNA polymerase with NifA, the transcriptional activator for nitrogen fixation operons. Cell **63:**11–22.
19. **Irons, R. D., and T. Sawahata.** 1985. Phenols, catechols, and quinones, p. 259–281. *In* M. W. Anders (ed.), Bioactivation of foreign compounds. Academic Press, Orlando, Fla.
20. **Jaspers, M. C. M., W. A. Suske, A. Schmid, D. A. M. Goslings, H.-P. E. Kohler, and J. R. van der Meer.** 2000. HbpR, a new member of the XylR/DmpR subclass within the NtrC family of bacterial transcriptional activators, regulates expression of 2-hydroxybiphenyl metabolism in *Pseudomonas azelaica* HBP1. J. Bacteriol. **182:**405–417.
21. **Kohler, H.-P. E., D. Kohler-Staub, and D. D. Focht.** 1988. Degradation of 2-hydroxybiphenyl and 2,2′-dihydroxybiphenyl by *Pseudomonas* sp. strain HBP1. Appl. Environ. Microbiol. **54:**2683–2688.
22. **Kohler, H.-P. E., A. Schmid, and M. van der Maarel.** 1993. Metabolism of 2,2′-dihydroxybiphenyl by *Pseudomonas* sp. strain HBP1: production and consumption of 2,2′,3-trihydroxybiphenyl. J. Bacteriol. **175:**1621–1628.
23. **Kohler, H.-P. E., M. J. E. C. van der Maarel, and D. Kohler-Staub.** 1993. Selection of *Pseudomonas* sp. strain HBP1 Prp for metabolism of 2-propylphenol and elucidation of the degradative pathway. Appl. Environ. Microbiol. **59:**860–866.
24. **Kristensen, C. S., L. Eberl, J. M. Sanchez-Romero, M. Givskov, S. Molin, and V. de Lorenzo.** 1995. Site-specific deletions of chromosomally located DNA segments with the multimer resolution system of broad-host-range plasmid RP4. J. Bacteriol. **177:**52–58.
25. **Kustu, S., A. K. North, and D. S. Weiss.** 1991. Prokaryotic transcriptional enhancers and enhancer-binding proteins. Trends Biochem. Sci. **16:**397–402.
26. **Kustu, S., E. Santero, J. Keener, D. Popham, and D. Weiss.** 1989. Expression of σ^{54} (*ntrA*)-dependent genes is probably united by a common mechanism. Microbiol. Rev. **53:**367–376.
27. **MacNeil, T., D. MacNeil, and B. Tyler.** 1982. Fine-structure deletion map and complementation analysis of the *glnA-glnL-glnG* region in *Escherichia coli*. J. Bacteriol. **150:**1302–1313.
28. **Mendelson, I., M. Gottesman, and A. B. Oppenheim.** 1991. HU and integration host factor function as auxiliary proteins in cleavage of phage lambda cohesive ends by terminase. J. Bacteriol. **173:**1670–1676.
29. **Morett, E., and L. Segovia.** 1993. The σ^{54} bacterial enhancer-binding protein family: mechanism of action and phylogenetic relationship of their functional domains. J. Bacteriol. **175:**6067–6074.
30. **Nakagawa, Y., and G. A. Moore.** 1995. Cytotoxic effects of postharvest fungicides, *ortho*-phenylphenol, thiabendazole and imazalil, on isolated rat hepatocytes. Life Sci. **57:**1433–1440.
31. **Nash, H. A.** 1996. The HU and IHF proteins: accessory factors for complex protein-DNA assemblies, p. 149–179. *In* E. C. C. Lin and A. S. Lynch (ed.), Regulation of gene expression in *Escherichia coli*. R. G. Landes Company, Austin, Tex.
32. **Ng, L. C., E. O'Neill, and V. Shingler.** 1996. Genetic evidence for interdomain regulation of the phenol-responsive σ^{54}-dependent activator DmpR. J. Biol. Chem. **271:**17281–17286.
33. **Pérez-Martín, J., and V. de Lorenzo.** 1995. The amino-terminal domain of the prokaryotic enhancer-binding protein XylR is a specific intramolecular repressor. Proc. Natl. Acad. Sci. USA **92:**9392–9396.
34. **Pérez-Martín, J., and V. de Lorenzo.** 1996. ATP binding to the σ^{54}-dependent activator XylR triggers a protein multimerization cycle catalyzed by UAS DNA. Cell **86:**331–339.
35. **Pérez-Martín, J., and V. de Lorenzo.** 1996. *In vitro* activities of an N-terminal truncated form of XylR, a σ^{54}-dependent transcriptional activator of *Pseudomonas putida*. J. Mol. Biol. **258:**575–587.
36. **Pérez-Martín, J., and V. de Lorenzo.** 1996. Physical and functional analysis of the prokaryotic enhancer of the σ^{54}-promoters of the TOL plasmid of *Pseudomonas putida*. J. Mol. Biol. **258:**562–574.
37. **Pérez-Martín, J., K. N. Timmis, and V. de Lorenzo.** 1994. Co-regulation by bent DNA. J. Biol. Chem. **269:**22657–22662.
38. **Porter, S. C., A. K. North, A. B. Wedel, and S. Kustu.** 1993. Oligomerization of NtrC at the *glnA* enhancer is required for transcriptional activation. Genes Dev. **7:**2258–2273.
39. **Ramos, J. L., S. Marqués, and K. N. Timmis.** 1997. Transcriptional control of the *Pseudomonas* TOL plasmid catabolic operons is achieved through an interplay of host factors and plasmid-encoded regulators. Annu. Rev. Microbiol. **51:**341–373.
40. **Ravatn, R., S. Studer, A. J. B. Zehnder, and J. R. van der Meer.** 1998. Int-B13, an unusual site-specific recombinase of the bacteriophage P4 integrase family, is responsible for chromosomal insertion of the 105-kilobase *clc* element of *Pseudomonas* sp. strain B13. J. Bacteriol. **180:**5505–5514.
41. **Ross, W., K. K. Gosink, J. Salomon, K. Igarashi, C. Zou, A. Ishihama, K. Severinov, and R. L. Gourse.** 1993. A third recognition element in bacterial promoters: DNA binding by the α subunit of RNA polymerase. Science **262:**1407–1413.
42. **Sambrook, J., E. F. Fritsch, and T. Maniatis.** 1989. Molecular cloning: a laboratory manual, 2nd ed. Cold Spring Harbor Laboratory Press, Cold Spring Harbor, N.Y.
43. **Schirmer, F., S. Ehrt, and W. Hillen.** 1997. Expression, inducer spectrum, domain structure, and function of MopR, the regulator of phenol degradation in *Acinetobacter calcoaceticus* NCIB8250. J. Bacteriol. **179:**1329–1336.
44. **Schmid, A.** 1997. Ph.D. thesis. Universität Stuttgart, Stuttgart, Germany.
45. **Shingler, V.** 1996. Signal sensing by σ^{54}-dependent regulators: derepression as a control mechanism. Mol. Microbiol. **19:**409–416.
46. **Shingler, V., M. Bartilson, and T. Moore.** 1993. Cloning and nucleotide sequence of the gene encoding the positive regulator (DmpR) of the phenol catabolic pathway encoded by pVI150 and identification of DmpR as a member of the NtrC family of transcriptional activators. J. Bacteriol. **175:**1596–1604.
47. **Sticher, P., M. C. M. Jaspers, K. Stemmler, H. Harms, A. J. B. Zehnder, and J. R. van der Meer.** 1997. Development and characterization of a whole-cell bioluminescent sensor for bioavailable middle-chain alkanes in contaminated groundwater samples. Appl. Environ. Microbiol. **63:**4053–4060.
48. **Suske, W. A., M. Held, A. Schmid, T. Fleischmann, M. G. Wubbolts, and H.-P. Kohler.** 1997. Purification and characterization of 2-hydroxybiphenyl 3-monooxygenase, a novel NADH-dependent, FAD-containing aromatic hydroxylase from *Pseudomonas azelaica* HBP1. J. Biol. Chem. **272:**24257–24265.
49. **Sze, C. C., T. Moore, and V. Shingler.** 1996. Growth phase-dependent transcription of the σ^{54}-dependent Po promoter controlling the *Pseudomonas*-derived (methyl)phenol *dmp* operon of pVI150. J. Bacteriol. **178:**3727–3735.
50. **Tayama, S., and Y. Nakagawa.** 1994. Effect of scavengers of active oxygen species on cell damage caused in CHO-K1 cells by phenylhydroquinone, an *o*-phenylphenol metabolite. Mutat. Res. **324:**121–131.
51. **van der Meer, J. R.** 1997. Evolution of novel metabolic pathways for the degradation of chloroaromatic compounds. Antonie Leeuwenhoek **71:**159–178.
52. **Wootton, J. C., and M. H. Drummond.** 1989. The Q-linker: a class of interdomain sequences found in bacterial multidomain regulatory proteins. Protein Eng. **2:**535–543.